Journal of Computational Applied Mechanics 2026, 57(1): 107-121

DOI: 10.22059/jcamech.2025.403575.1634

RESEARCH PAPER

Free axial and torsional vibration of boron nitride nanorods using nonlocal finite element method

Aleyna Yazıcıoğlu [a], Ömer Civalek [a,b,*]

[a] *Civil Engineering Department, Division of Mechanics, Akdeniz University, Antalya 07070, Türkiye*
[b] *Department of Medical Research, China Medical University, Taichung, Taiwan*

Abstract

In this study, the formulation of nonlocal finite elements is developed for nanorods under axial and torsional vibrations using nonlocal elasticity theory. First, an overview of the topic is provided along with review of relevant studies in literature. Next, the fundamental formulations of nonlocal elasticity theory are presented, and the corresponding equations of motion for axial and torsional vibrations are derived. Based on these formulations, the stiffness and polar inertia matrices of the nanorod are obtained using the weighted residual method. Finally, the numerical results are illustrated through graphical representations, highlighting the effects of nanorod length, the number of finite elements, and the nonlocal parameters.

Keywords: Nonlocal elasticity, finite element method, vibration, boron nitride nanorods

1. Introduction

Nanostructures are utilized in various forms such as nanowire, nanorod, nanoring, and nanoplate across a wide range of fields including sensors, biomedical engineering, electronics, computer technology, aerospace and defense within the scope of nanoelectromechanical systems (NEMS). Due to the wide range of applications, investigating the static and dynamic behavior of these structures is crucial for achieving reliable designs and ensuring long-term durability. For this purpose, numerous researchers have investigated nanostructures since their emergence, and the key contributions in this area are summarized below from various aspects.

In 1959, Richard Feynman said in a speech, “If materials and devices can be made at the molecular level, this will be the source of new discoveries.” This statement can be considered as the first step towards nanoscience and nanotechnology. Subsequent breakthroughs such as the invention of the scanning tunnelling microscope (STM) in 1981, the discovery of the C_{60} molecule in 1985, the development of atomic force microscopy (AFM) in 1986, and the discovery of carbon nanotubes (CNTs) in 1991 increased interest in this field. In parallel with these advances, higher-order elasticity theories were developed to provide a more accurate analysis of the mechanical behavior of nanostructures [1-3]. Eringen’s nonlocal theory [4-6] is one of the most prominent higher-order elasticity theories and has been widely applied to various problems. For example, it has been used to investigate the axial buckling behavior of multi-walled carbon nanotubes [7], their transverse free vibrations [8], and wave propagation in CNTs using two models of nonlocal continuum mechanics: the elastic Euler–Bernoulli and Timoshenko beam models [9]. The bending

* Corresponding author. Tel.: +90-242-310-6319; fax: +90-242-310-6306.
E-mail address: civalek@yahoo.com

wave propagation of single-walled CNTs has been analyzed using the Timoshenko beam model [10], while their bending and buckling behavior has been examined with the Euler–Bernoulli beam model [11, 12]. The buckling behavior of micro and nanorods/tubes was also investigated with the Timoshenko beam models [13].
The scope of nonlocal elasticity theory has been further expanded through its application to the analysis of nanoscale structures under various geometries and boundary conditions. Such as the buckling and vibration of nanoplates using Navier- and Levy-type solutions [14], the axial vibration of nanorods and single-walled CNTs embedded in elastic media [15], the torsional statics and dynamics of CNTs within elastic matrices [16], and the torsional vibration of double-walled CNTs considering van der Waals interactions [17]. The axial free vibration of functionally graded tapered nanorods was investigated using the theory of nonlocal elasticity. The results obtained were also compared with those obtained from classical theory [18]. In addition to CNTs, boron nitride (BNNTs) and silicon carbide nanotubes (SiCNTs) have also been discovered [19, 20]. The atomic structure of the boron nitride layer has a hexagonal arrangement and consists of boron (B) and nitrogen (N) atoms. Similarly, the silicon carbide structure also consists of silicon (Si) and carbon (C) atoms. The bond length between boron and nitrogen atoms is approximately 1.46 Å, while the bond length between silicon and carbon atoms is approximately 1.94 Å (see Fig 1).

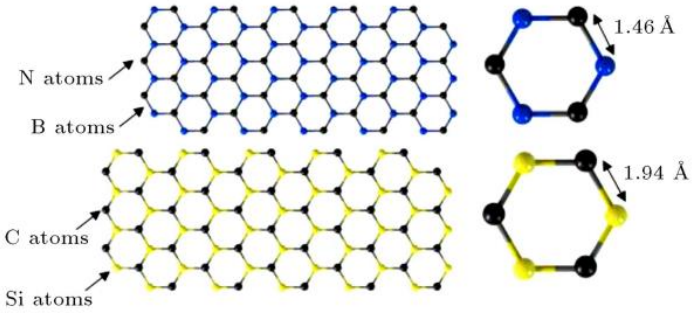

Fig 1: Atomic structure of boron nitride and silicon carbide sheets [21] .

BNNTs offer several advantages over CNTs in various aspects. They have higher chemical stability, thermal resistance and elasticity modules. Depending on the tube's radius and chirality, CNTs can be conductive or semiconductive, while BNNTs always exhibit insulating properties, independent of tube morphology and chirality [22]. They can be integrated into polymer matrices more easily than CNTs. Thanks to these properties, they open the door to numerous new applications. Furthermore, it has been reported that BNNTs have a very high potential for transporting drug molecules into the bloodstream by binding to them [23]. For these reasons, BNNTs, which are considered an advanced material in technological developments, have become the focus of numerous studies in recent years. The free vibration behavior of the sandwich plate with CNTs and BNNTs reinforced cores was investigated and a comparative analysis was carried out to evaluate the effects of these reinforcements on the vibration characteristics of the composite plate[24]. Similarly, BNNTs and SiCNTs have been comparatively analyzed using the strain gradient Euler–Bernoulli beam theory [25].
The nonlocal finite element method (NL-FEM) represents another widely used approach for investigating the mechanical behavior of nanostructures. A variety of problems have been analyzed using this framework, and the results have shown good agreement with those reported in the literature [26-30]. A free vibration analysis of CNTs and SiCNTs embedded in an elastic matrix was carried out using Eringen's nonlocal elasticity theory and Hermite polynomials within the finite element formulation, under different boundary conditions [31]. A four-node finite element model was developed using Lagrangian and Hermitian interpolation functions for the bending and free vibration analysis of functionally graded (FG) nanoplates resting on elastic foundations [32]. The vibration behavior of FG nanobeam composed of alumina (Al_2O_3) and steel under various boundary conditions was investigated using NL-FEM and the effect of the foundation was investigated by considering a single parameter Winkler type elastic foundation model in the problem [33]. In a similar study, the size-effect free vibration behavior of functionally graded (FG) curvilinear Euler–Bernoulli nanobeams resting on Winkler foundations was analyzed using the finite element formulation developed within the framework of two-phase local/non-local models [34]. Nonlocal free vibration analysis of axial rods embedded in elastic media was performed using the Love-Bishop rod theory with the finite element method [35]. In another study, the free vibration behavior of porous functionally graded nanoplates was investigated by combining the Rayleigh–Ritz approach with the NL-FEM method [36]. In a study, a new curvilinear finite element based on two-node and exact analytical solutions is proposed to analyze the in-plane static behavior of curvilinear nanobeams, unlike traditional finite elements based on approximate interpolation functions [37]. After a certain point, studies have aimed to analyze nanoscale structures more precisely by developing higher-order nonlocal theories [38-44]. In one study, analysis was performed using Piola peridynamics and Eringen nonlocal elasticity together for particle-based materials [45], and in another study, the Eringen model used for bounded continuum media

was developed for both bounded and unbounded structures [46]. The vibration behavior of porous nanobeams was investigated with Levinson beam theory, nonlocal elasticity theory, and machine learning (ML) techniques [47]. A new theory called modified nonlocal strain gradient theory was established for the analysis of functionally graded nanosheets. The analysis of porous FG microbeams under moving load is solved based on Bernoulli–Euler beam and modified couple stress theories [48]. The dynamic behavior of truncated conical baskets rotating around two independent axes has been investigated. The conical basket was reinforced by CNT and its mechanical properties were determined based on different distribution types of CNTs. An innovative approach to dynamic analysis has been proposed for these conical baskets, which are like perforated centrifuge structures in application [49]. Some comparative studies were conducted to determine the accuracy and reliability of the proposed theory in specific situations [50]. Torsional vibrations of noncircular nanorods with varying boundary conditions were investigated using second-order strain gradient theory. Furthermore, cross-sectional deflection due to the noncircular cross-sectional area of the nanorod was also considered in the calculations [51]. Torsion and bending analysis of sandwich beams were carried out with various beam theories [52]. Thermoelastic vibrations of a nonlocal medium subjected to pulsed heat flux was analyzed with an improved model [53]. The static pull-in response of a micro switch under longitudinal magnetic field was obtained using nonlocal couple stress theory and Galerkin method [54]. In another study, the magneto-electro vibration of sandwich panel reinforced with porous core and graphene sheets was considered according to nonlocal strain gradient theory [55]. Similarly, free vibration and stability analyses of sandwich pipe with fluid-conveyed were studied according to Timoshenko beam theory [56]. The size-effect vibration behavior of a dielectric elastomer microbeam resonator was investigated using the Cosserat continuum model and for this purpose, the equation of motion of the system was obtained using the Hamilton principle and the Galerkin method [57]. Vibration analysis of Timoshenko sandwich beams with symmetric and asymmetric distributions on the material surfaces was performed using both nonlocal stress and strain parameters. Combining these two concepts yields a nonlocal stress-strain elasticity theory, and the analysis results show that the natural frequency is higher when only the nonlocal stress parameter is considered and lower when only the nonlocal strain parameter is considered [58].
Research on the analysis of nanostructures continues in the literature, depending on complex material systems and ambient conditions. These studies enhance the understanding of the mechanical, thermal, and electrical properties of nanostructures and contribute to the development of more efficient and durable materials in engineering applications. This study provides a theoretical framework for understanding the size-dependent axial and torsional vibration characteristics of boron nitride nanorods, one of the promising materials for technological advancement. The main innovation of this study is the formulation of a nonlocal finite element model that simultaneously derives the axial and torsional vibrations of BNNTs within the same theoretical framework. In the study, the stiffness matrix, classical polar inertia matrix and nonlocal polar inertia matrix are obtained and the role of nonlocal effects on dynamic behavior is investigated. In addition, nanorod length, the effects of nonlocal parameters and number of finite elements for axial and torsional vibrations are analyzed and the results are presented by means of graphs.

2. Theory and Formulations

2.1. Nonlocal Elasticity Theory

Classical elasticity theories have been found inadequate for analyzing the mechanical behavior of nanoscale structures due to their neglect size effects. To provide a more accurate model nanoscale structures, nonlocal theories have been developed. One such theory, Eringen's nonlocal elasticity theory, defines the nonlocal stress at any point z as follows [59]:

$$\sigma_{kl}(z) = \int_V \alpha(|z' - z|, \chi)\, C_{kl}(z') dV(z') \tag{1}$$

$$C_{kl}(z') = \lambda \varepsilon_{ii}(z') \delta_{kl} + 2\mu \varepsilon_{kl}(z') \tag{2}$$

$$\varepsilon_{kl}(z') = \frac{1}{2}\left(\frac{\partial u_k(z')}{\partial z_l'} + \frac{\partial u_l(z')}{\partial z_k'}\right) \tag{3}$$

In the equations given above, σ_{kl} is the nonlocal stress tensor, $\alpha|z - z'|$ is the distance in Euclidean form, $C_{kl}(z')$ local stress tensor of the body at point z', V is the volume occupied by the elastic body, λ and μ are Lamé constants, $\varepsilon_{kl}(z')$ is the linear strain tensor of the body at point z', $u_{k,l}$ is the displacement vector of the body for any reference point z'. In contrast to the classical elasticity theory, this theory provides a more realistic mechanical model by considering interatomic interactions. This interaction is represented by the expression χ in Eq. (1).

$$\chi = \frac{e_0 a}{l} \tag{4}$$

Here, e_0 is the experimentally determined material constant, a is the internal interatomic distance, and l external characteristic length of the material. The nonlocal parameter $(e_0 a)$ defines the scale of long-range interactions between atoms in a continuum. As $e_0 a$ increases, the stress at a point is affected by strains across a larger region. Consequently, since the size effects of nanoscale structures are considered, their dynamic and static behaviors can be analyzed with higher accuracy.

The integral constitutive relation given in Eqs. (1-3) creates difficulties in analyzing elasticity problems. Therefore, an equivalent differential form of this expression was developed to analyze different problems. The differential form was expressed by Eringen as follows [5]:

$$[1 - (e_0 a)^2 \nabla^2]\sigma_{kl} = C_{kl} \tag{5}$$

here, ∇^2 is the Laplacian.

2.2. Axial and Torsional Vibration

In this section, the equation of motion of the nanorod under free axial and torsional vibration will be derived using the nonlocal theory of elasticity. For this purpose, consider the displacement and rotation of a nanorod extending along z-axis at any time t be denoted as $u(z,t)$ and $\theta(z,t)$ respectively (Fig 2).

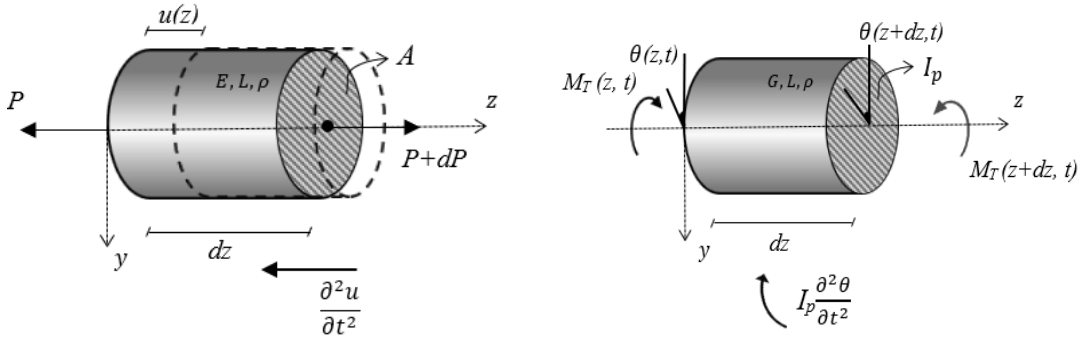

Fig 2: Differential element of a nanorod under axial (a) and torsional (b) vibration.

Eq. (5) can be reformulated, as only the axial force P and the torsional moment M_T arise along the nanorod axis for axial and torsional vibrations, respectively.

$$P - (e_0 a)^2 \frac{\partial^2 P}{\partial z^2} = EA \frac{\partial u}{\partial z} \tag{6}$$

$$M_T - (e_0 a)^2 \frac{\partial^2 M_T}{\partial z^2} = GI_p \frac{\partial \theta}{\partial z} \tag{7}$$

Here, E is the elastic modulus, G is the shear modulus, A is the cross-sectional area and $I_p = I_p(z)$ is the polar moment of inertia of the cross-sectional area at z with respect to the center. For axial and torsional vibrations in a continuous system, the following expressions can also be defined:

$$\frac{\partial P}{\partial z} = \rho A \frac{\partial^2 u}{\partial t^2} \tag{8}$$

$$\frac{\partial M_T}{\partial z} = \rho I_p \frac{\partial^2 \theta}{\partial t^2} \tag{9}$$

Here, ρ is the mass density. Substituting Eq. (8) into Eq. (6) and then Eq. (9) into Eq. (7), the following equations of motion are obtained for both types of vibration.

$$EA\frac{\partial^2 u}{\partial z^2} - \rho A\frac{\partial^2 u}{\partial t^2} + (e_0 a)^2 \rho A\frac{\partial^4 u}{\partial z^2 \partial t^2} = 0 \tag{10}$$

$$GI_p\frac{\partial^2 \theta}{\partial z^2} - \rho I_p\frac{\partial^2 \theta}{\partial t^2} + (e_0 a)^2 \rho I_p\frac{\partial^4 \theta}{\partial z^2 \partial t^2} = 0 \tag{11}$$

The above given equations are reformulated into eigenvalue problems using the method of separation of variables. These eigenvalue problems are then solved under the boundary conditions of the nanorod, yielding the natural frequencies and the corresponding mode shapes.

2.3. Nonlocal Finite Element Method

The finite element method (FEM) relies on the use of approximate functions to obtain results that are close to the exact solution. In the exact analysis of torsional and axial vibration problems, the right-hand side of the governing equations must vanish. However, in approximate methods, this condition cannot be strictly satisfied. To address this, the FEM employs the weighted residual approach, which minimizes the average residual. Accordingly, the expressions are given in Eqs. (10) and (11) are multiplied by a weighting function $w(z, y)$ and integrated over the length of the nanorod.

$$I = \int_0^L wR dz \tag{12}$$

If partial integration is applied to each term of the obtained equations, the weak formulation of the differential equation for axial vibration can be derived as follows:

$$I = w\left(EA\frac{\partial u}{\partial z} + (e_0 a)^2 \rho A\frac{\partial^3 u}{\partial z \partial t^2}\right)\Big|_0^L - \int_0^L \left[EA\frac{\partial w}{\partial z}\frac{\partial u}{\partial z} + w\rho A\frac{\partial^2 u}{\partial t^2} + (e_0 a)^2 \rho A\frac{\partial w}{\partial z}\frac{\partial^3 u}{\partial z \partial t^2}\right] dz \tag{13}$$

For torsional vibration:

$$I = w\left(GI_p\frac{\partial \theta}{\partial z} + (e_0 a)^2 \rho I_p\frac{\partial^3 \theta}{\partial z \partial t^2}\right)\Big|_0^L - \int_0^L \left[GI_p\frac{\partial w}{\partial z} + w\rho I_p\frac{\partial^2 \theta}{\partial t^2} + (e_0 a)^2 \rho I_p\frac{\partial w}{\partial z}\frac{\partial^3 \theta}{\partial z \partial t^2}\right] dz \tag{14}$$

Under the prescribed boundary conditions, the boundary terms in Eqs. (13) and (14) vanish, and the weak form of the equations is obtained. The finite element formulation of a two-node rod element, in terms of the displacement and rotation at nodes i and j is expressed as follows:

$$u(z) = [N_1 \quad N_2]\begin{Bmatrix} u_i \\ u_j \end{Bmatrix},\ \theta(z) = [N_1 \quad N_2]\begin{Bmatrix} \theta_i \\ \theta_j \end{Bmatrix} \tag{15}$$

$$N_1 = \left(1 - \frac{z}{L}\right), \quad N_2 = \frac{z}{L} \tag{16}$$

Additionally, some transformations are made to rearrange the equations.

$$\begin{aligned} &w = N^T,\ \frac{\partial w}{\partial z} = B^T \\ &\frac{\partial u}{\partial z} = Bu,\ \frac{\partial \theta}{\partial z} = B\theta \\ &B = D^k N \\ &\frac{\partial^2 u}{\partial t^2} = N\ddot{u},\ \frac{\partial^2 \theta}{\partial t^2} = N\ddot{\theta} \end{aligned} \tag{17}$$

Here $D^k = \partial(*)/\partial z$ represents kinematic operator, N denotes the shape function vector, while $\ddot{u}$ and $\ddot{\theta}$ represent displacement and angular acceleration, respectively. If Eqs. (13) and (14) are rearranged using these expressions:

$$\int_0^L EA(B^T B)u\, dz + \int_0^L \rho A[(e_0 a)^2 B^T B + N^T N]\,\ddot{u}\, dz = 0 \tag{18}$$

$$\int_0^L GI_p(B^TB)\theta\, dz + \int_0^L \rho I_p[(e_0a)^2B^TB + N^TN]\,\ddot{\theta}\, dz = 0 \tag{19}$$

Eqs. (18) and (19) in general form are as follows:

$$K\{u,\theta\} + [I_c + I_{nl}]\{\ddot{u},\ddot{\theta}\} = 0 \tag{20}$$

$$K = \begin{cases} \frac{EA}{L}\begin{bmatrix} 1 & -1 \\ -1 & 1 \end{bmatrix} \\ \frac{GI_p}{L}\begin{bmatrix} 1 & -1 \\ -1 & 1 \end{bmatrix} \end{cases},\ I_c = \begin{cases} \frac{\rho AL}{6}\begin{bmatrix} 2 & 1 \\ 1 & 2 \end{bmatrix} \\ \frac{\rho I_pL}{6}\begin{bmatrix} 2 & 1 \\ 1 & 2 \end{bmatrix} \end{cases},\ I_{nl} = \begin{cases} \frac{\rho A(e_0a)^2}{L}\begin{bmatrix} 1 & -1 \\ -1 & 1 \end{bmatrix} \\ \frac{\rho I_p(e_0a)^2}{L}\begin{bmatrix} 1 & -1 \\ -1 & 1 \end{bmatrix} \end{cases} \tag{21}$$

Here K is the stiffness matrix of the finite element, I_c is the classical polar inertia and I_{nl} is the nonlocal polar inertia matrix. If the transformation $e^{i\omega t}$ is applied to Eq. (20), the following equation is obtained, and the frequency values can be found at the roots of this equation.

$$|[K] - \omega^2[I_c + I_{nl}]| = 0 \tag{22}$$

In the most general case for a system divided into n parts:

$$K = \left\{ n\ x\ \left(\frac{EA}{L}, \frac{GI_p}{L}\right) \begin{bmatrix} 1 & -1 & 0 & 0 & . & . & . & 0 & 0 \\ -1 & 2 & -1 & 0 & . & . & . & 0 & 0 \\ 0 & -1 & 2 & -1 & . & . & . & 0 & 0 \\ 0 & 0 & -1 & 2 & . & . & . & 0 & 0 \\ . & . & . & . & . & . & . & 0 & 0 \\ . & . & . & . & . & . & . & -1 & 0 \\ 0 & 0 & 0 & 0 & 0 & 0 & -1 & 2 & -1 \\ 0 & 0 & 0 & 0 & 0 & 0 & 0 & -1 & 1 \end{bmatrix}_{n+1\ x\ n+1} \right. \tag{23}$$

$$I_c = \left\{ \frac{1}{n}\ x\ \left(\frac{\rho AL}{6}, \frac{\rho I_pL}{6}\right) \begin{bmatrix} 2 & 1 & 0 & 0 & . & . & . & 0 & 0 \\ 1 & 4 & 1 & 0 & . & . & . & 0 & 0 \\ 0 & 1 & 4 & 1 & . & . & . & 0 & 0 \\ 0 & 0 & 1 & 4 & . & . & . & 0 & 0 \\ . & . & . & . & . & . & . & 0 & 0 \\ . & . & . & . & . & . & . & 1 & 0 \\ 0 & 0 & 0 & 0 & 0 & 0 & 1 & 4 & 1 \\ 0 & 0 & 0 & 0 & 0 & 0 & 0 & 1 & 2 \end{bmatrix}_{n+1\ x\ n+1} \right. \tag{24}$$

$$I_{nl} = \left\{ n\ x\ \left(\frac{\rho A(e_0a)^2}{L}, \frac{\rho I_p(e_0a)^2}{L}\right) \begin{bmatrix} 1 & -1 & 0 & 0 & . & . & . & 0 & 0 \\ -1 & 2 & -1 & 0 & . & . & . & 0 & 0 \\ 0 & -1 & 2 & -1 & . & . & . & 0 & 0 \\ 0 & 0 & -1 & 2 & . & . & . & 0 & 0 \\ . & . & . & . & . & . & . & 0 & 0 \\ . & . & . & . & . & . & . & -1 & 0 \\ 0 & 0 & 0 & 0 & 0 & 0 & -1 & 2 & -1 \\ 0 & 0 & 0 & 0 & 0 & 0 & 0 & -1 & 1 \end{bmatrix}_{n+1\ x\ n+1} \right. \tag{25}$$

3. Numerical Results and Discussion

In this study, the axial and torsional vibration behaviors of BNNTs are investigated using the NL-FEM based on Eringen's nonlocal elasticity theory. The stiffness and polar inertia matrices of the nanorods are formulated to explicitly incorporate the influence of nonlocal parameters. Numerical results are performed for different nanorod lengths, numbers of finite elements, and nonlocal parameter values. The mechanical and geometric properties used in the analysis are presented in Table 1.

Table 1: Geometric and mechanical properties of the BNNTs [60, 61]

Geometric Properties	
Nanorod length (L)	25-100 (nm)

Circular cross-section diameter (D)	1-5 (nm)
Nonlocal parameter (e_0a)	0-25 (nm)
Mechanical Properties	
Mass density (ρ)	2270 (kg/m^3)
Poisson's ratio (υ)	0.2
Elastic modulus (E)	1.22 (TPa)
Shear modules (G)	0.50 (TPa)

In this table, the shear modulus was calculated using the classical elasticity theory through the relation $G = \frac{E}{2(1+\upsilon)}$, and was found to be approximately $0.50\ TPa$. The nondimensional frequency parameter used in numerical analyses is defined as $\dot{\omega} = \frac{\omega L}{\sqrt{E/\rho}}$ for axial vibration and $\dot{\omega} = \frac{\omega L}{\sqrt{G/\rho}}$ for torsional vibration, where ω denotes the natural frequency. Furthermore, the nondimensional nonlocal parameter is expressed as $\xi = \frac{e_0 a}{L}$.

The calculated deviation values for all modes are quite low, which clearly reveals that the proposed nonlocal FEM formulation has high accuracy and convergence.

Table 2 compares the values of the first three natural frequencies obtained in the present study with those reported in Ref. [62]. The computations were performed for the dimensionless nonlocal parameter $\xi = 0$ (classical) and $\xi = 0.2$, using $n = 100$ elements. Similarly, the torsional frequencies are compared in Table 3 with Ref. [27]. In this context, the values $e_0a = 0$ (classical), $e_0a = 5$ and $e_0a = 10$ for the nonlocal parameter are considered. As can be seen, the results obtained in both cases are in extremely good agreement with the references.

Additionally, the percentage deviation between the current FEM results and the reference values is calculated as follows to evaluate the accuracy of the results:

$$\delta(\%) = \frac{|\omega_{FEM} - \omega_{Ref}|}{\omega_{Ref}} x100 \tag{26}$$

The calculated deviation values for all modes are quite low, which clearly reveals that the proposed nonlocal FEM formulation has high accuracy and convergence.

Table 2: Comparison of the first three frequencies value.

C-C Mode Number	Present ($n = 100$) THz	Ref. [62] ($\xi = 0$) THz	$\delta(\%)$	Present ($n = 100$) THz	Ref. [62] ($\xi = 0.2$) THz	$\delta(\%)$
1	0.2410	0.2410	0	0.2041	0.2041	0
2	0.4821	0.4821	0	0.3002	0.3002	0
3	0.7234	0.7231	0.04	0.3389	0.3389	0
C-F Mode Number	Present ($n = 100$) THz	Ref. [62] ($\xi = 0$) THz	$\delta(\%)$	Present ($n = 100$) THz	Ref. [62] ($\xi = 0.2$) THz	$\delta(\%)$
1	0.1205	0.1205	0	0.1149	0.1150	0.09
2	0.3616	0.3615	0.03	0.2631	0.2631	0
3	0.6027	0.6026	0.02	0.3236	0.3236	0

Table 3: Comparison of the first three frequencies value.

C-C Mode Number	Present ($n = 100$) THz	Ref. [27] ($e_0a = 0$) THz	$\delta(\%)$	Present ($n = 100$) THz	Ref. [27] ($e_0a = 5$) THz	$\delta(\%)$	Present ($n = 100$) THz	Ref. [27] ($e_0a = 10$) THz	$\delta(\%)$
1	0.4265	0.4285	0.47	0.3354	0.3370	0.47	0.2290	0.2301	0.48
2	0.8531	0.8570	0.45	0.4581	0.4603	0.48	0.2587	0.2600	0.50
3	1.2800	0.2856	0.44	0.4910	0.5022	2.23	0.2656	0.2669	0.49
C-F Mode Number	Present ($n = 100$) THz	Ref. [27] ($e_0a = 0$) THz	$\delta(\%)$	Present ($n = 100$) THz	Ref. [27] ($e_0a = 5$) THz	$\delta(\%)$	Present ($n = 100$) THz	Ref. [27] ($e_0a = 10$) THz	$\delta(\%)$
1	0.2133	0.2143	0.47	0.1985	0.1994	0.45	0.1678	0.1685	0.42

2	0.6398	0.6428	0.47	0.4140	0.4160	0.48	0.2410	0.2511	4.02
3	1.0665	1.0713	0.45	0.4839	0.4862	0.47	0.2631	0.2644	0.49

To investigate the effect of the dimensionless nonlocal parameter (ξ), the variation in natural frequency values corresponding to different ξ values and mode numbers is presented in Fig 3 for axial vibration. As seen in the figures, an increase in the nonlocal effect leads to a decrease in the natural frequency values. This trend is observed for both clamped–clamped (C–C) and clamped–free (C–F) boundary conditions. Nevertheless, due to the higher stiffness provided by the double clamping, the frequency values are greater under the C–C boundary condition.

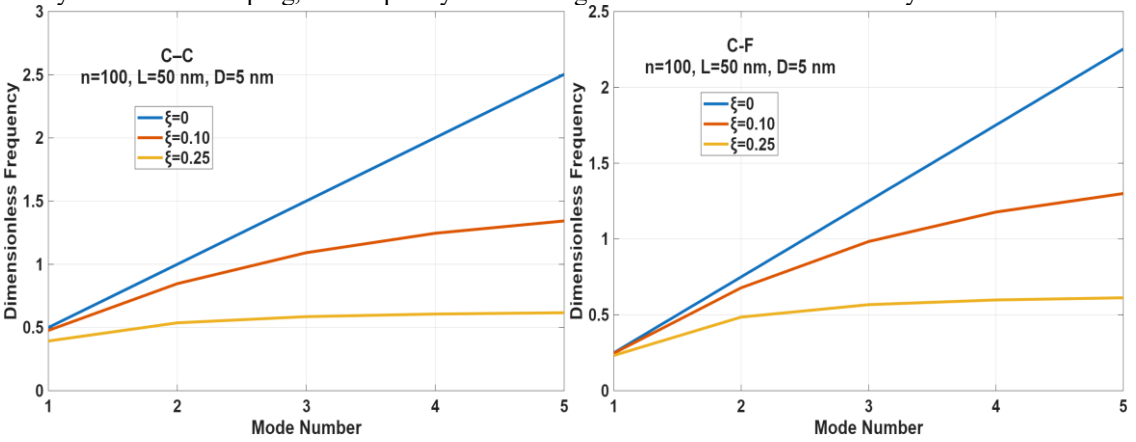

Fig 3: Effect of nonlocal parameter on the dimensionless frequency of a nanotube under different boundary conditions.

Fig 4 illustrates the influence of nanorod length on axial and torsional vibration frequencies under both C–C and C–F boundary conditions. As the rod length increases, the natural frequencies decrease due to the reduction in structural stiffness, while higher mode numbers yield larger frequency values, consistent with classical vibration theory. The axial vibration frequencies are considerably higher than the torsional ones, reflecting the greater resistance of the nanorod to axial deformation. Similarly, the C–C boundary condition produces higher frequency values than the C–F condition across all cases, highlighting influence of boundary conditions on dynamic behavior.

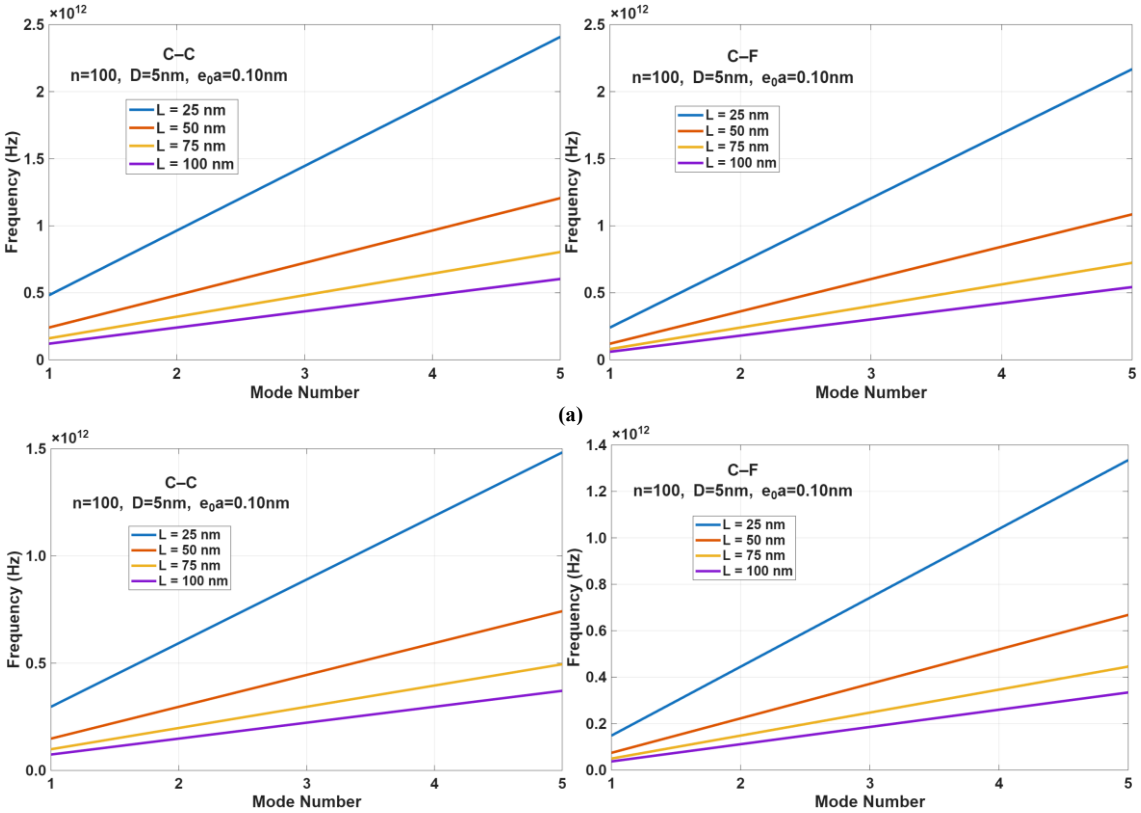

(b)

Fig 4: Axial (a) and torsional (b) vibration frequencies of a nanorod under C–C and C–F boundary conditions for different rod lengths.

The results obtained with the FEM are directly dependent on the number of elements used in the system. Especially in the determination of natural frequencies, low element numbers may cause errors, while the results obtained by increasing the number of elements become more stable and reliable.

Table 4 and Fig 5 presents the axial and torsional vibration frequencies (THz) of a nanotube under C–C and C–F boundary conditions for different element numbers (n) using the NL-FEM. As the number of elements increases, the computed frequencies converge toward stable values, demonstrating that mesh refinement enhances numerical accuracy. It is evident that axial vibration frequencies are considerably higher than torsional ones, owing to the greater structural stiffness against axial deformation. Furthermore, the C–C boundary condition yields higher frequency values compared to the C–F condition across all mode numbers, underscoring the influence of boundary constraints on dynamic behavior. Additionally, the natural frequency increases with mode number, as expected from classical vibration theory. These findings confirm the validity and sensitivity of the NL-FEM approach in capturing the vibrational characteristics of nanoscale rods under various mechanical constraints.

Table 4: Axial and torsional vibration frequencies for various element numbers under C–C and C–F boundary conditions ($L = 50\ nm, D = 5\ nm, e_0a = 0.25\ nm$)

		Axial Vibration			Torsional Vibration		
Mode Number		1	2	3	1	2	3
BCs	n	THz	THz	THz	THz	THz	THz
C-C	10	0.2420	0.4898	0.7492	0.1490	0.3016	0.4613
	25	0.2412	0.4831	0.7266	0.1485	0.2975	0.4474
	50	0.2410	0.4821	0.7234	0.1484	0.2969	0.4454
	100	0.2410	0.4819	0.7226	0.1484	0.2967	0.4449
	101	0.2410	0.4819	0.7225	0.1484	0.2967	0.4449
C-F	10	0.1206	0.3648	0.6177	0.0743	0.2246	0.3803
	25	0.1205	0.3620	0.6046	0.0742	0.2229	0.3723
	50	0.1205	0.3616	0.6027	0.0742	0.2226	0.3711
	100	0.1205	0.3615	0.6023	0.0742	0.2226	0.3708
	101	0.1205	0.3615	0.6023	0.0742	0.2226	0.3708

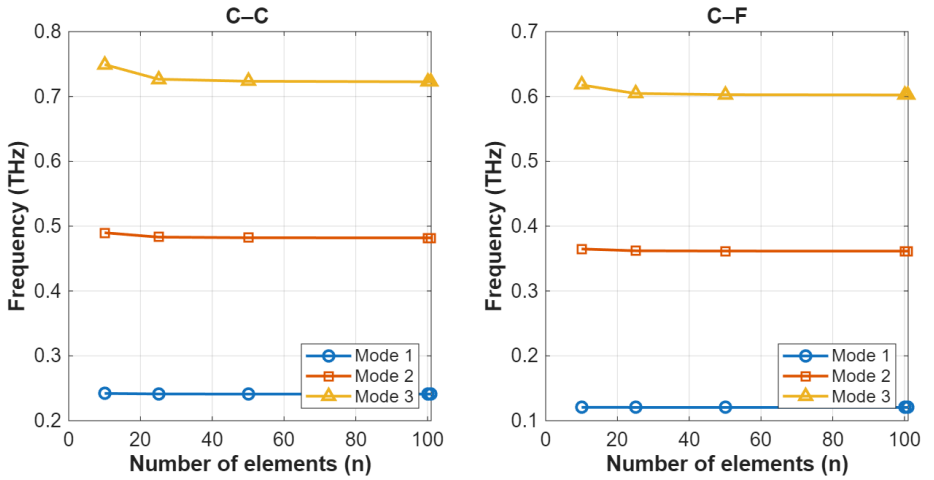

(a)

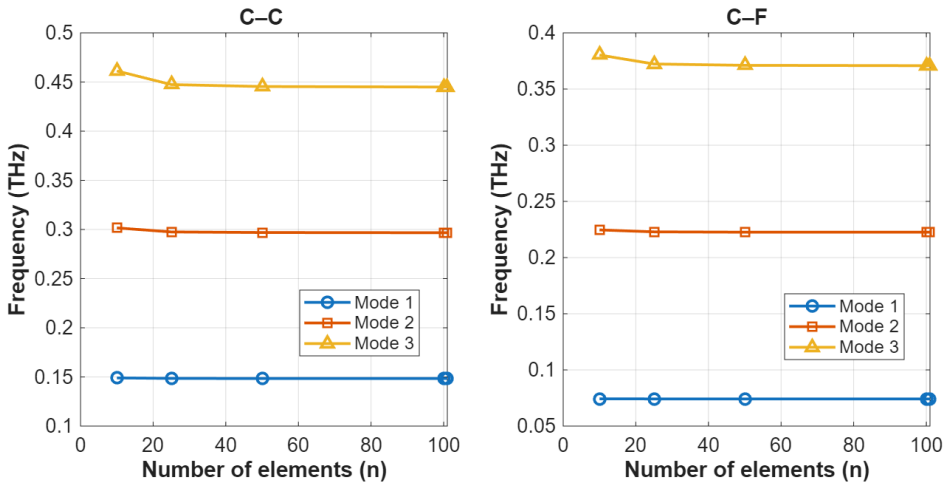

Fig 5: Axial (a) and torsional (b) vibration frequencies for various element numbers under C–C and C–F boundary conditions.

Fig 6 presents two separate graphs showing the variation of axial and torsional vibration frequencies with respect to the mode number and the n .As can be seen, as the number of elements increases, significant differences in frequency values occur in the upper modes, while this difference remains limited in the lower modes. This suggests that higher-frequency modes are more sensitive to mesh resolution.

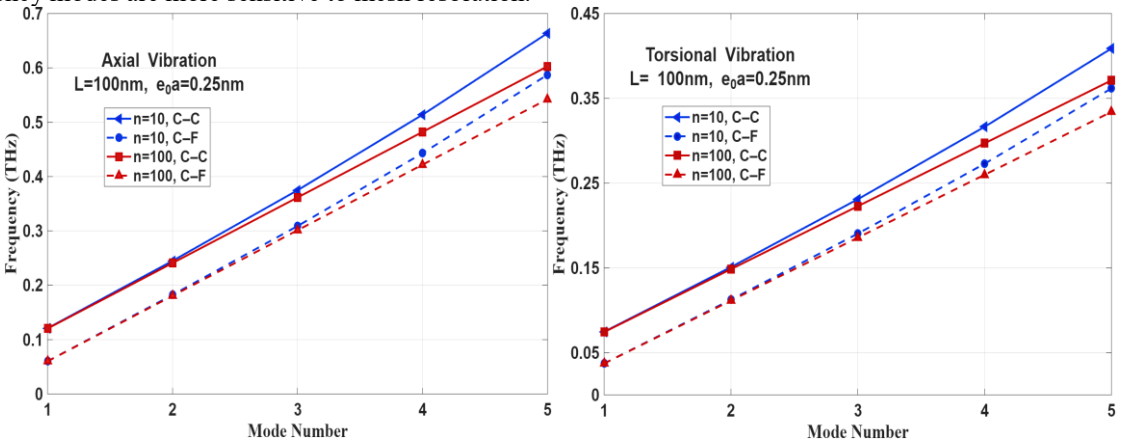

Fig 6: Axial (a) and torsional (b) vibration frequencies of a nanorod under C–C and C–F boundary conditions for different rod length.

Table 5 shows the effect of the nonlocal parameter on natural frequencies for different nanorod diameters. As can be seen from the table, changing the nanorod diameter has no effect on the frequency values. This is due to the simplification of the cross-sectional area A or the polar moment of inertia I_p in the frequency expressions. Therefore, for uniform (constant cross-section) nanorods, it is expected that the cross-sectional diameter has no effect on frequencies. However, when there is a geometric change along the cross-section (e.g., a taper or variable radius), the diameter change will have a significant effect on the natural frequencies.

Furthermore, consistent with the graphical results in Fig 3, as clearly seen in the table, natural frequency values decrease as the value of the nonlocal parameter increases. This is due to the decrease in effective stiffness due to the inclusion of internal interactions within the material in the nonlocal theory. In other words, increasing distant interactions at the atomic scale causes the system to behave more flexibly, thus decreasing natural frequencies.

Table 5: Axial and torsional vibration frequencies for various diameter of nanorod and nonlocal parameter under C–C boundary condition ($L = 20\ nm,\ n = 100$)

			Axial Vibration			Torsional Vibration		
BCs	Mode $[THz]$	Nonlocal parameter (e_0a) $[nm]$	Diameter of nanorod (D) $[nm]$			Diameter of nanorod (D) $[nm]$		
			1	3	5	1	3	5

C-C	ω_1	0	0.2410	0.2410	0.2410	0.1414	0.1414	0.1414
		3	0.2369	0.2369	0.2369	0.1390	0.1390	0.1390
		5	0.2299	0.2299	0.2299	0.1349	0.1349	0.1349
	ω_2	0	0.4821	0.4821	0.4821	0.2829	0.2829	0.2829
		3	0.4511	0.4511	0.4511	02647	02647	02647
		5	0.4082	0.4082	0.4082	0.2395	0.2395	0.2395
	ω_3	0	0.7234	0.7234	0.7234	0.4244	0.4244	0.4244
		3	0.6296	0.6296	0.6296	0.3694	0.3694	0.3694
		5	0.5263	0.5263	0.5263	0.3088	0.3088	0.3088

Fig 7 presents the first five axial and torsional mode shapes of the nanorod under the C–C and C–F boundary conditions. To obtain the mode shapes, the expressions for $u(z,t)$ and $\theta(z,t)$ in equation (20) were assumed to exhibit harmonic motion, and the transformations $u(z,t) = U(z)e^{iwt}$ and $\theta(z,t) = \theta(z)e^{iwt}$ were applied accordingly. As a result of this assumption, an eigenvalue problem determining the mode shapes was obtained and solved numerically. In the C–C case, the mode shapes satisfy the zero-displacement condition at both ends, while in the C–F case, the amplitude increases at the free end. A similar situation applies to the rotation angles. As can be seen from the figure, the number of waves increases in all cases as the number of modes increases.

Although the distribution of $\theta(z)$ in torsional vibration is similar in mathematical form to the axial displacement $U(z)$, their physical interpretations differ axial vibration represents longitudinal extension and contraction of the nanorod, whereas torsional vibration corresponds to the angular rotation of the cross-section about its axis.

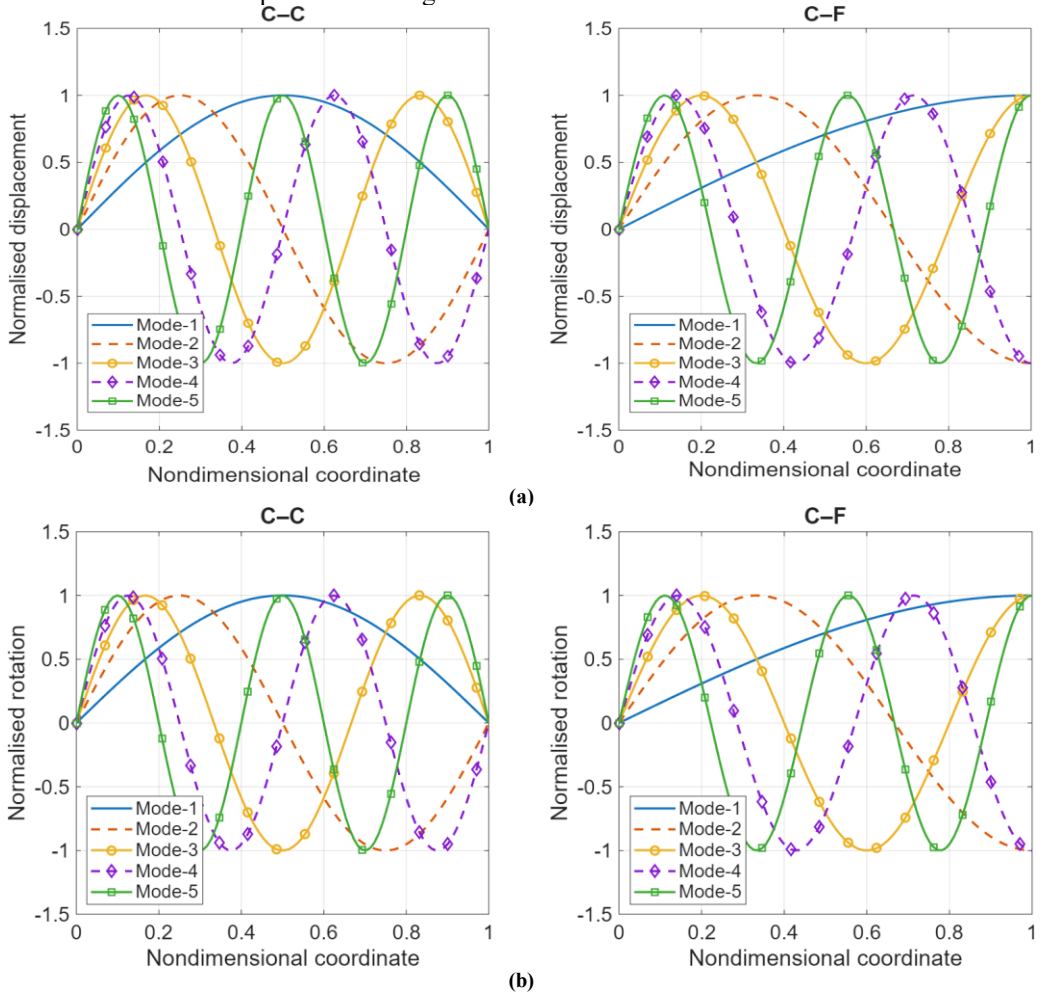

Fig 7:First five axial (a) and torsional (b) mode shapes of the nanorod under C-C and C-F boundary conditions.

4. Conclusions

In this study, the axial and torsional vibration response of boron nitride nanorods is analyzed using the NL-FEM based on Eringen's nonlocal elasticity theory. The governing equations are derived for both vibration types, and corresponding finite element formulations are developed to incorporate nonlocal effects into the inertia matrices. Numerical results are presented graphically to evaluate the influence of nanorod length, nonlocal parameter, element number, and boundary conditions on natural frequencies. The key findings obtained from this study are summarized as follows:

- An increase in the nonlocal parameter leads to a significant reduction in both axial and torsional natural frequencies, highlighting the importance of small-scale effects on the dynamic behavior of nanorods.
- The increase in nanorod length leads to a significant decrease in the natural frequencies for all modes, and this effect is observed under both C–C and C–F boundary conditions.
- The C–C boundary condition produced higher frequency values compared to the C–F condition, which reveals the effect of the boundary conditions on the stiffness.
- As the number of finite elements increases (n), the computed natural frequency values converge to stable results, emphasizing the impact of mesh refinement on the accuracy of numerical computations. Furthermore, as n increases, the initial modes remain almost unchanged, while the higher modes show significant changes.
- The axial vibration frequencies are observed to be higher than the torsional frequencies, which can be attributed to the substantially greater axial stiffness of the nanorod compared to its torsional stiffness.
- Since the cross-sectional area simplifies in the natural frequency equations, the change in the diameter of the nanorod does not have any effect on the natural frequency values.
- The mode shape of the nanorod is unaffected by the nonlocal parameter but varies with the number of modes.

Future work plans to extend the model to include complex geometries and different boundary conditions. BNNTs are advanced materials with the potential for use in various engineering and nanotechnological applications under different geometric structures and loading conditions. Furthermore, developing the model to include additional physical effects such as thermal loads, viscoelastic damping, and composite nanorod configurations will contribute to a more realistic representation of behavior at the nanoscale. The findings from this study are expected to provide a computational reference for experimental validation studies and molecular dynamics simulations to be performed on boron nitride nanostructures.

References

[1] A. C. Eringen, D. Edelen, On nonlocal elasticity, *International journal of engineering science,* Vol. 10, No. 3, pp. 233-248, 1972.

[2] C. Lim, G. Zhang, J. Reddy, A higher-order nonlocal elasticity and strain gradient theory and its applications in wave propagation, *Journal of the Mechanics and Physics of Solids,* Vol. 78, pp. 298-313, 2015.

[3] F. Yang, A. Chong, D. C. C. Lam, P. Tong, Couple stress based strain gradient theory for elasticity, *International journal of solids and structures,* Vol. 39, No. 10, pp. 2731-2743, 2002.

[4] A. C. Eringen, Plane waves in nonlocal micropolar elasticity, *International Journal of Engineering Science,* Vol. 22, No. 8-10, pp. 1113-1121, 1984.

[5] A. C. Eringen, Nonlocal polar elastic continua, *International journal of engineering science,* Vol. 10, No. 1, pp. 1-16, 1972.

[6] A. C. Eringen, Theory of thermomicrofluids, *Journal of Mathematical analysis and Applications,* Vol. 38, No. 2, pp. 480-496, 1972.

[7] Y. Zhang, G. Liu, J. Wang, Small-scale effects on buckling of multiwalled carbon nanotubes under axial compression, *Physical Review B—Condensed Matter and Materials Physics,* Vol. 70, No. 20, pp. 205430, 2004.

[8] Y. Zhang, G. Liu, X. Xie, Free transverse vibrations of double-walled carbon nanotubes using a theory of nonlocal elasticity, *Physical Review B—Condensed Matter and Materials Physics,* Vol. 71, No. 19, pp. 195404, 2005.

[9] Q. Wang, Wave propagation in carbon nanotubes via nonlocal continuum mechanics, *Journal of Applied physics,* Vol. 98, No. 12, 2005.

[10] L. Wang, H. Hu, Flexural wave propagation in single-walled carbon nanotubes, *Physical Review B—Condensed Matter and Materials Physics,* Vol. 71, No. 19, pp. 195412, 2005.

[11] Ö. Civalek, Ç. Demir, B. Akgöz, Static analysis of single walled carbon nanotubes (SWCNT) based on Eringen's nonlocal elasticity theory, *International Journal of Engineering and Applied Sciences,* Vol. 1, No. 2, pp. 47-56, 2009.

[12] O. Civalek, C. Demir, Buckling and bending analyses of cantilever carbon nanotubes using the Euler-Bernoulli beam theory based on non-local continuum model; technical note, 2011.

[13] C. Wang, Y. Zhang, S. S. Ramesh, S. Kitipornchai, Buckling analysis of micro-and nano-rods/tubes based on nonlocal Timoshenko beam theory, *Journal of Physics D: Applied Physics,* Vol. 39, No. 17, pp. 3904, 2006.

[14] T. Aksencer, M. Aydogdu, Levy type solution method for vibration and buckling of nanoplates using nonlocal elasticity theory, *Physica E: Low-dimensional Systems and Nanostructures,* Vol. 43, No. 4, pp. 954-959, 2011.

[15] M. Aydogdu, Axial vibration analysis of nanorods (carbon nanotubes) embedded in an elastic medium using nonlocal elasticity, *Mechanics Research Communications,* Vol. 43, pp. 34-40, 2012.

[16] M. Arda, M. Aydogdu, Torsional statics and dynamics of nanotubes embedded in an elastic medium, *Composite Structures,* Vol. 114, pp. 80-91, 2014.

[17] M. Aydogdu, M. Arda, Torsional vibration analysis of double walled carbon nanotubes using nonlocal elasticity, *International Journal of Mechanics and Materials in Design,* Vol. 12, No. 1, pp. 71-84, 2016.

[18] M. Şimşek, Nonlocal effects in the free longitudinal vibration of axially functionally graded tapered nanorods, *Computational Materials Science,* Vol. 61, pp. 257-265, 2012.

[19] K. Mercan, Ö. Civalek, Buckling analysis of Silicon carbide nanotubes (SiCNTs) with surface effect and nonlocal elasticity using the method of HDQ, *Composites Part B: Engineering,* Vol. 114, pp. 34-45, 2017.

[20] B. Uzun, H. Numanoglu, O. Civalek, Free vibration analysis of BNNT with different cross-Sections via nonlocal FEM, *Journal of Computational Applied Mechanics,* Vol. 49, No. 2, pp. 252-260, 2018.

[21] H. Numanoglu, K. Mercan, Ö. Civalek, Finite element model and size-dependent stability analysis of boron nitride and silicon carbide nanowires/nanotubes, *Scientia Iranica,* Vol. 26, No. 4, 2019.

[22] A. O. Maselugbo, H. B. Harrison, J. R. Alston, Boron nitride nanotubes: a review of recent progress on purification methods and techniques, *Journal of Materials Research,* Vol. 37, No. 24, pp. 4438-4458, 2022.

[23] H. Xu, Q. Wang, G. Fan, X. Chu, Theoretical study of boron nitride nanotubes as drug delivery vehicles of some anticancer drugs, *Theoretical Chemistry Accounts,* Vol. 137, No. 7, pp. 104, 2018.

[24] Z. K. Maraghi, A. G. Arani, O. Civalek, Comparative analysis of carbon and boron-nitride nanotube reinforcements on the vibration characteristics of magnetostrictive sandwich plates, *Composite Structures,* Vol. 361, pp. 119029, 2025.

[25] A. Tepe, Comparative size-dependent free vibration analysis of boron nitride and silicon carbide nanotubes based on strain gradient Euler–Bernoulli beam theory, *Mechanics Based Design of Structures and Machines*, pp. 1-21, 2025.

[26] J. Phadikar, S. Pradhan, Variational formulation and finite element analysis for nonlocal elastic nanobeams and nanoplates, *Computational materials science,* Vol. 49, No. 3, pp. 492-499, 2010.

[27] H. M. Numanoğlu, Ö. Civalek, On the torsional vibration of nanorods surrounded by elastic matrix via nonlocal FEM, *International Journal of Mechanical Sciences,* Vol. 161, pp. 105076, 2019.

[28] A. Yazıcıoğlu, Ö. Civalek, Axial Vibration of a Nanoring Rod Using Nonlocal Finite Element Method, *International Journal of Engineering and Applied Sciences,* Vol. 17, No. 2, pp. 73-80, 2025.

[29] M. Eltaher, S. A. Emam, F. Mahmoud, Free vibration analysis of functionally graded size-dependent nanobeams, *Applied Mathematics and Computation,* Vol. 218, No. 14, pp. 7406-7420, 2012.

[30] M.-O. Belarbi, S. Benounas, L. Li, P. Van Vinh, A. Garg, Vibration of a functionally graded doubly curved shallow nanoshell: an improved FSDT model and its nonlocal finite element implement, *Journal of Vibration Engineering & Technologies,* Vol. 13, No. 1, pp. 93, 2025.

[31] Ö. Civalek, B. Uzun, M. Ö. Yaylı, B. Akgöz, Size-dependent transverse and longitudinal vibrations of embedded carbon and silica carbide nanotubes by nonlocal finite element method, *The European Physical Journal Plus,* Vol. 135, No. 4, pp. 381, 2020.

[32] V.-K. Tran, Q.-H. Pham, T. Nguyen-Thoi, A finite element formulation using four-unknown incorporating nonlocal theory for bending and free vibration analysis of functionally graded nanoplates resting on elastic medium foundations, *Engineering with Computers,* Vol. 38, No. 2, pp. 1465-1490, 2022.

[33] B. Uzun, Ö. Civalek, M. Ö. Yaylı, Vibration of FG nano-sized beams embedded in Winkler elastic foundation and with various boundary conditions, *Mechanics Based Design of Structures and Machines,* Vol. 51, No. 1, pp. 481-500, 2023.

[34] Y. Tang, P. Bian, H. Qing, Finite element formulation for free vibration of the functionally graded curved nonlocal nanobeam resting on nonlocal elastic foundation, *Journal of Vibration and Control*, pp. 10775463241278642, 2024.

[35] Ö. Civalek, H. M. Numanoğlu, Nonlocal finite element analysis for axial vibration of embedded love–bishop nanorods, *International Journal of Mechanical Sciences,* Vol. 188, pp. 105939, 2020.

[36] A. S. Kumar, S. Kumar, P. K. Choudhary, A. Gupta, A. Narayan, Free vibration characteristics of elastic foundation-supported porous functionally graded nanoplates using Rayleigh-Ritz approach, *International Journal of Structural Integrity,* Vol. 15, No. 2, pp. 298-321, 2024.

[37] Ö. E. Genel, H. Koç, E. Tüfekci, In-Plane Static Analysis of Curved Nanobeams Using Exact-Solution-Based Finite Element Formulation, *Computers, Materials & Continua,* Vol. 82, No. 2, 2025.

[38] Q.-H. Pham, V. K. Tran, T. T. Tran, V. C. Nguyen, A. M. Zenkour, Nonlocal higher-order finite element modeling for vibration analysis of viscoelastic orthotropic nanoplates resting on variable viscoelastic foundation, *Composite Structures,* Vol. 318, pp. 117067, 2023.

[39] H. Koc, E. Tufekci, A novel approach of bending behavior of carbon nanotubes by combining the effects of higher-order boundary conditions and coupling through doublet mechanics, *Mechanics of Advanced Materials and Structures,* Vol. 31, No. 27, pp. 8905-8919, 2024.

[40] E. Yıldırım, I. Esen, Effect of the porous structure on the hygrothermal vibration analysis of functional graded nanoplates using nonlocal high-order continuum plate model, *Acta Mechanica,* Vol. 235, No. 8, pp. 5079-5106, 2024.

[41] A. E. Abouelregal, Ö. Civalek, B. Akgöz, A size-dependent non-fourier heat conduction model for magneto-thermoelastic vibration response of nanosystems, *Journal of Applied and Computational Mechanics,* Vol. 11, No. 2, pp. 344-357, 2025.

[42] D. M. Lan, N. D. Anh, P. V. Dong, D. V. Thom, Ö. Civalek, P. V. Minh, A new Galerkin method for buckling of sandwich nanobeams, *Proceedings of the Institution of Mechanical Engineers, Part C: Journal of Mechanical Engineering Science,* Vol. 239, No. 8, pp. 3034-3051, 2025.

[43] M. S. Vaccaro, R. Luciano, F. Marotti de Sciarra, Size-dependent stress-driven behaviour of nanobeams based on higher-order theories, *Meccanica*, pp. 1-22, 2025.

[44] M. Akpınar, B. Uzun, H. G. Kadıoğlu, M. Ö. Yaylı, Dynamics of a Short-Fiber-Reinforced Nanorod via Hardening Nonlocal Approach, *Mechanics of Solids*, pp. 1-23, 2025.

[45] G. La Valle, C. Soize, A higher-order nonlocal elasticity continuum model for deterministic and stochastic particle-based materials, *Zeitschrift für angewandte Mathematik und Physik,* Vol. 75, No. 2, pp. 49, 2024.

[46] R. Barretta, R. Luciano, F. M. de Sciarra, M. S. Vaccaro, Modelling issues and advances in nonlocal beams mechanics, *International Journal of Engineering Science,* Vol. 198, pp. 104042, 2024.

[47] A. Tariq, B. Uzun, B. Deliktaş, M. Ö. Yaylı, Application of machine learning methodology for investigating the vibration behavior of functionally graded porous nanobeams, *The Journal of Strain Analysis for Engineering Design,* Vol. 60, No. 2, pp. 131-151, 2025.

[48] Ş. D. Akbaş, S. Dastjerdi, B. Akgöz, Ö. Civalek, Dynamic analysis of functionally graded porous microbeams under moving load, *Transport in Porous Media,* Vol. 142, No. 1, pp. 209-227, 2022.

[49] S. Dastjerdi, Ö. Civalek, M. Malikan, B. Akgöz, On analysis of nanocomposite conical structures, *International Journal of Engineering Science,* Vol. 191, pp. 103918, 2023.

[50] P. Van Vinh, A novel modified nonlocal strain gradient theory for comprehensive analysis of functionally graded nanoplates, *Acta Mechanica,* Vol. 236, No. 1, pp. 173-204, 2025.

[51] Ö. Civalek, M. Akpınar, B. Uzun, M. Ö. Yaylı, Dynamics of a non-circular-shaped nanorod with deformable boundaries based on second-order strain gradient theory, *Archive of Applied Mechanics,* Vol. 94, No. 11, pp. 3555-3572, 2024.

[52] M. Mehdi, Buckling and bending analyses of a sandwich beam based on nonlocal stress-strain elasticity theory with porous core and functionally graded facesheets, *Advances in materials research: AMR,* Vol. 11, No. 4, pp. 279-298, 2022.

[53] A. E. Abouelregal, B. Akgöz, Ö. Civalek, Nonlocal thermoelastic vibration of a solid medium subjected to a pulsed heat flux via Caputo–Fabrizio fractional derivative heat conduction, *Applied Physics A,* Vol. 128, No. 8, pp. 660, 2022.

[54] M. Mahdavi Adeli, R. Mahmoudi, A. Soleimani, Pull-in behaviour of a micro switch actuated by the electrostatic under a uniform longitudinal magnetic field based on nonlocal couple stress theory, *Journal of Computational Applied Mechanics,* Vol. 54, No. 4, pp. 577-587, 2023.

[55] M. A. Mohammadimehr, A. Loghman, S. Amir, M. Mohammadimehr, E. Arshid, Ö. Civalek, Magneto-electro vibration analysis of a moderately thick double-curved sandwich panel with porous core and GPLRC using FSDT, *Journal of Computational Applied Mechanics,* Vol. 56, No. 3, pp. 673-693, 2025.

[56] M. Nejadi, M. Mohammadimehr, M. Mehrabi, Free vibration and stability analysis of sandwich pipe by considering porosity and graphene platelet effects on conveying fluid flow, *Alexandria Engineering Journal,* Vol. 60, No. 1, pp. 1945-1954, 2021.

[57] A. Alibakhshi, S. Dastjerdi, B. Akgöz, Ö. Civalek, Parametric vibration of a dielectric elastomer microbeam resonator based on a hyperelastic cosserat continuum model, *Composite Structures,* Vol. 287, pp. 115386, 2022.

[58] M. Mohammadimehr, The effect of a nonlocal stress-strain elasticity theory on the vibration analysis of Timoshenko sandwich beam theory, *Advances in nano research,* Vol. 17, No. 3, pp. 275-284, 2024.

[59] A. C. Eringen, *On differential equations of nonlocal elasticity and solutions of screw dislocation and surface waves*, pp. 1983.

[60] N. G. Chopra, A. Zettl, Measurement of the elastic modulus of a multi-wall boron nitride nanotube, *Solid State Communications,* Vol. 105, No. 5, pp. 297-300, 1998.

[61] L. Jiang, W. Guo, A molecular mechanics study on size-dependent elastic properties of single-walled boron nitride nanotubes, *Journal of the Mechanics and Physics of Solids,* Vol. 59, No. 6, pp. 1204-1213, 2011.

[62] U. Uyan, *Yerel Olmayan Elastisite Teorisi İle Bor Nitrür Nanoçubukların Eksenel Titreşimi*, Master Degree Thesis, Civil Engeenering, Akdeniz Univercity, Turkey, 2018.